Physiological and cell morphology adaptation of Bacillus subtilis at near-zero specific growth rates

Overkamp, Wout; Ercan, Onur; Herber, Martijn; van Maris, Antonius J. A.; Kleerebezem, Michiel; Kuipers, Oscar P.

Published in:
Environmental Microbiology

DOI:
10.1111/1462-2920.12676

environmental microbiology

Environmental Microbiology (2015) **17**(2), 346–363 doi:10.1111/1462-2920.12676

Physiological and cell morphology adaptation of *Bacillus subtilis* at near-zero specific growth rates: a transcriptome analysis

Wout Overkamp,[1,2] Onur Ercan,[2,3,4] Martijn Herber,[1] Antonius J. A. van Maris,[2,5] Michiel Kleerebezem[2,3,6] and Oscar P. Kuipers[1,2*]

[1]*Department of Molecular Genetics, Groningen Biomolecular Sciences and Biotechnology Institute, University of Groningen, Nijenborgh 7, 9747 AG Groningen, The Netherlands.*

[2]*Kluyver Centre for Genomics of Industrial Fermentation, P.O. Box 5057, 2600 GA Delft, The Netherlands.*

[3]*NIZO food research, P.O. Box 20, 6710 BA Ede, The Netherlands.*

[4]*Laboratory of Microbiology, Wageningen University, P.O. Box 8033, 6700 EJ Wageningen, The Netherlands.*

[5]*Department of Biotechnology, Delft University of Technology, Julianalaan 67, 2628 BC Delft, The Netherlands.*

[6]*Host Microbe Interactomics Group, Wageningen University, De Elst 1, 6708 WD Wageningen, The Netherlands.*

Summary

Nutrient scarcity is a common condition in nature, but the resulting extremely low growth rates (below 0.025 h^{-1}) are an unexplored research area in *Bacillus subtilis*. To understand microbial life in natural environments, studying the adaptation of *B. subtilis* to near-zero growth conditions is relevant. To this end, a chemostat modified for culturing an asporogenous *B. subtilis sigF* mutant strain at extremely low growth rates (also named a retentostat) was set up, and biomass accumulation, culture viability, metabolite production and cell morphology were analysed. During retentostat culturing, the specific growth rate decreased to a minimum of 0.00006 h^{-1}, corresponding to a doubling time of 470 days. The energy distribution between growth and maintenance-related processes showed that a state of near-zero growth was reached. Remarkably, a filamentous cell morphology emerged, suggesting that cell separation is impaired under near-zero growth conditions. To evaluate the corresponding molecular adaptations to extremely low specific growth, transcriptome changes were analysed. These revealed that cellular responses to near-zero growth conditions share several similarities with those of cells during the stationary phase of batch growth. However, fundamental differences between these two non-growing states are apparent by their high viability and absence of stationary phase mutagenesis under near-zero growth conditions.

Received 16 July, 2014; revised 10 October, 2014; accepted 16 October, 2014. *For correspondence. E-mail o.p.kuipers@rug.nl; Tel. (+31) 503632093; Fax (+31) 503632348.

Introduction

Microbial growth is determined by available nutrient concentrations, and in nature, nutrient availability varies over time and per environment (Koch, 1971; Demoling *et al.*, 2007). Regardless of whether the environment facilitates a feast and famine lifestyle (Koch, 1971) or an oligotrophic existence (Egli, 2010), the concentrations of assimilable substrates are frequently low but not absolutely zero (Ferenci, 2001). Consequently, the specific growth rate of most microorganisms is far below their maximum during the vast majority of time. High microbial growth rates as achieved in laboratory batch cultures are probably rare in nature (Brock, 1971; Koch, 1997; Ferenci, 2001). Therefore, to better understand microbial life in natural environments, knowledge about physiology at near-zero growth rates is very relevant.

Inside the cell of a microorganism, numerous biological processes take place that require energy. These cellular processes can be categorized into growth and non-growth-related processes. The former involve reactions contributing to production of new cell constituents as well as synthesis of the machineries required for cell division. The latter are also referred to as maintenance processes, and involve reactions associated with functions other than biomass formation (e.g. maintenance of chemi-osmotic potential and turnover of macromolecular compounds; van Bodegom, 2007). When nutrients are present in excess and environmental conditions are favourable, microorganisms invest the majority of the available metabolic energy in growth. In nutrient-limiting conditions

however, a relatively large fraction of the energy sources has to be used for maintenance-related processes (Pirt, 1965; Nyström, 2004a; van Bodegom, 2007). When the metabolic energy distribution between growth and maintenance has come to a point where available energy is spent exclusively on non-growth associated processes, zero-growth is the result.

Zero-growth is a metabolically active, non-growing state of a microorganism and is fundamentally different from starvation encountered during stationary phase, which involves deterioration of physiological processes. The energetic investment for an organism to remain in a viable and active state without growth is quantified by the so-called non-growth-associated maintenance energy coefficient (Pirt, 1965). Resting states as typified by spores, which have little or no metabolic activity, are not considered to be in zero-growth state.

Even in well-studied organisms such as *Bacillus subtilis*, extremely slow growth has not been investigated extensively, mostly due to a lack of experimental accessibility to achieve near-zero growth rates (Pirt, 1987). For example, in batch cultivations, where cells proliferate at their maximum growth rates until nutrients are depleted, the transition from exponential to stationary phase is rapid and involves continuously changing environmental conditions.

Chemostat cultivation allows growth under controlled environmental conditions and at submaximal specific growth rates. The growth rate can be manipulated by varying the dilution rate, making the chemostat a proven set-up for studying the effect of growth rate on physiology (Novick and Szilard, 1950; Herbert *et al*., 1956; Sauer *et al*., 1996; Dauner *et al*., 2001). However, due to homogeneity problems at low dilution rates caused by the dropwise feeding of medium, specific growth rates lower than 0.025 h^{-1} cannot be set up reliably in chemostats (Herbert *et al*., 1956; Daran-Lapujade *et al*., 2009).

To be able to study microbial physiology at extremely low specific growth rates, retentostat cultivation has been developed (Herbert, 1961; van Verseveld *et al*., 1986). A retentostat, or recycling fermentor, is a chemostat in which all the biomass is retained in the fermenter vessel by a filter in the effluent line. Growing a culture at a fixed dilution rate on an energy-limited medium leads to accumulation of biomass and a progressive decrease of energy substrate availability per cell. Consequently, energy available for growth becomes more and more limiting, ultimately leading to zero-growth rates when the substrate consumption rate equals the substrate requirements for maintenance processes. Meanwhile, starvation is prevented in this set-up because the substrate supply continues (Herbert, 1961; Chesbro *et al*., 1979; van Verseveld *et al*., 1986; Tappe *et al*., 1996; Boender *et al*., 2009; Goffin *et al*., 2010; Ercan *et al*., 2013).

From previously conducted long-term retentostat cultivation studies (22–45 days) it was concluded that *Saccharomyces cerevisiae* (Boender *et al*., 2009), *Lactobacillus plantarum* (Goffin *et al*., 2010) and *Lactococcus lactis* (Ercan *et al*., 2013) exhibit energy distribution and maintenance characteristics that can be predicted from higher growth rate chemostats. This is in contrast with studies on *Escherichia coli* (Chesbro *et al*., 1979), *Bacillus polymyxa* (Arbige and Chesbro, 1982), *Paracoccus denitrificans* and *Bacillus licheniformis* (van Verseveld *et al*., 1986), which applied short-term set-ups (3 days) not truly allowing zero-growth conditions to establish.

The physiology of *B. subtilis* at various specific growth rates has been the subject of numerous studies (Sauer *et al*., 1996; Dauner *et al*., 2001; Tännler *et al*., 2008; Blom *et al*., 2011). However, retentostat studies with specific growth rates that approximate zero are an unexplored area in the *B. subtilis* field. *Bacillus subtilis* is found in a large variety of niches, like soil and water, in which zero-growth is probably a common state. The differentiation strategies that *B. subtilis* has evolved, such as formation of highly resistant spores, development of natural competence and motility, secretion of exoproteases and biofilm formation (Dubnau, 1991; Msadek, 1999; Branda *et al*., 2001; Errington, 2003; Kearns and Losick, 2005; Veening *et al*., 2008) are probably a reflection of its habitat flexibility. They facilitate survival under a large variety of (dynamic) environmental conditions, making it an intriguing subject of study.

Here, we describe the cultivation of an asporogenous *B. subtilis sigF* mutant strain in an aerobic, glucose-limited retentostat with the aim to investigate the physiological and transcriptional responses to near-zero specific growth rates. The *sigF* mutant strain is used to prevent undesirable sporulation/germination processes, which would interfere with reaching near-zero growth rates. During these long-term retentostat cultivations, extremely low growth rates were reached, and remarkable cell morphology changes emerged. The caloric restriction encountered during retentostat cultivation clearly was reflected in the *B. subtilis* transcriptome, which established that adaptations to extremely low growth rates display similarity to cells that are progressing from growing to non-growing growth phases in a batch culture. However, the transcriptome analyses also indicated that the slow progressive transition towards the non-growing state in a retentostat with controlled environmental conditions yields a condition fundamentally different from the abrupt entry into stationary phase. In this non-growing state, the assumption is that cryptic growth, e.g. the lysis of cells that are replaced at the same rate by the growth of others (Ryan, 1959), is very limited. Consequently, growth-related genome mutation rates (mutations arising during

deoxyribonucleic acid (DNA) replication within actively dividing cells) are most likely not very numerous (Drake, 1991; Drake *et al*., 1998; Barrick *et al*., 2009). Therefore, genome sequencing was used to corroborate that very limited numbers of mutations are found in the zero-growth cultures.

Results

Implementation of aerobic retentostat cultivation for B. subtilis

Defining the experimental set-up for retentostat cultivation of *B. subtilis* required a number of modifications relative to other zero-growth studies (Boender *et al*., 2009; Ercan *et al*., 2013). Because sporulation will interfere with reaching a zero-growth state and therefore is undesired, a sporulation-deficient *sigF* mutant was used in this study. This strain can initiate sporulation, but is unable to express the genes necessary for continuation of the process at stage II in the sporulation cascade (Piggot and Coote, 1976; Setlow *et al*., 1991; Dworkin and Losick, 2005). The use of a knockout strain may impose a limitation in terms of being able to interpret the natural response of the organism. However, this particular mutant is still able to express genes for sporulation initiation (Fawcett *et al*., 2000; Steil *et al*., 2005; Wang *et al*., 2006) and thereby still allows us to see if sporulation is one of the responses *B. subtilis* applies. For retentostat cultivation, bioreactors (Fig. 1) were equipped with a large filtration surface cross-flow filter to minimize the risk of clogging during cultivation (Koros *et al*., 1996). Complete biomass retention was confirmed by regular plating of effluent. Continuous filtration for up to 42 days was possible without noticeable clogging or observation of growth in the effluent. Due to the fusion of green fluorescent protein (GFP) with the promoter of the constitutively expressed *rrnB* gene, contamination could be distinguished from the GFP-expressing *B. subtilis* cells. The retentostat cultures described here did not experience any contamination. Growth of *B. subtilis* in medium-supply tubing was found to be a potential problem during prolonged (> 7 days) cultivation. To prevent growth in the tubing, a dropper was installed between the medium inlet and the medium-supply tubing, preventing direct contact. Foaming was prevented most effectively by automatically supplying anti-foam on regular intervals. For a more detailed description of the retentostat set-up, see supplementary material.

Growth and viability in retentostat cultures

Bacillus subtilis 168 *trpC2 sigF::spec amyE::*P*rrnB*-GFP was grown under aerobic retentostat conditions in chemically defined M9 medium with glucose as the growth-limiting substrate. Two independent retentostat cultivations were successfully performed for 42 and 40 days (retentostat 1 and 2, respectively) to study the adaptation of *B. subtilis* to near-zero specific growth rates.

Biomass (measured in grams dry weight (g_{dw})) accumulated in the bioreactor and asymptotically levelled off to a near zero growth state during a total of approximately 20 days (Fig. 2A). During this period, the calculated specific growth rate (μ) decreased from 0.025 h^{-1} to 0.0004 h^{-1} (Fig. 2A). At the end of the cultivation, after approximately 40 days, a minimum was reached of 0.00006 h^{-1}. The specific growth rate reached at the end of the cultivation corresponded to a doubling time of approximately 470 days.

The biomass accumulation in the retentostat cultivations can be modelled with the van Verseveld equation

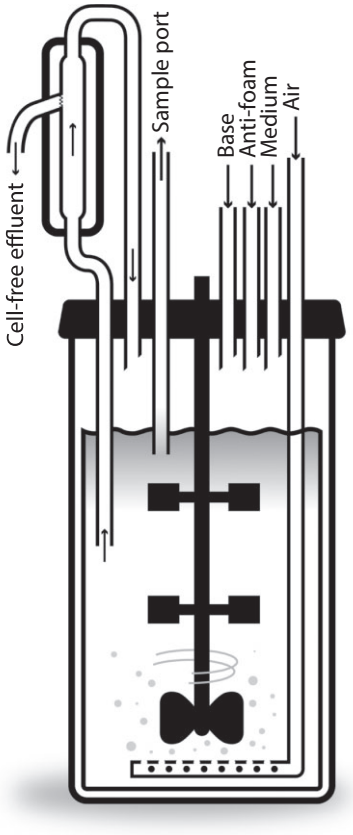

Fig. 1. Schematic illustration of a retentostat. A constant flow of air and fresh medium is provided to the culture. Anti-foam is added with timed intervals to prevent foaming. Biomass is retained in the reactor by a cross-flow filter on the effluent line. By means of a pump, the culture is circulated over the filter loop to prevent clogging and deoxygenation in the filter. Not displayed in the figure are the DO, pH, temperature and level sensors used for monitoring of the culture. The pH sensor is coupled to the base feed to maintain a constant pH. Upon contact of the culture with the level sensor, cell-free effluent is pumped out of the reactor to keep a constant culture volume. Samples are withdrawn directly from the culture using an aseptic sampler system.

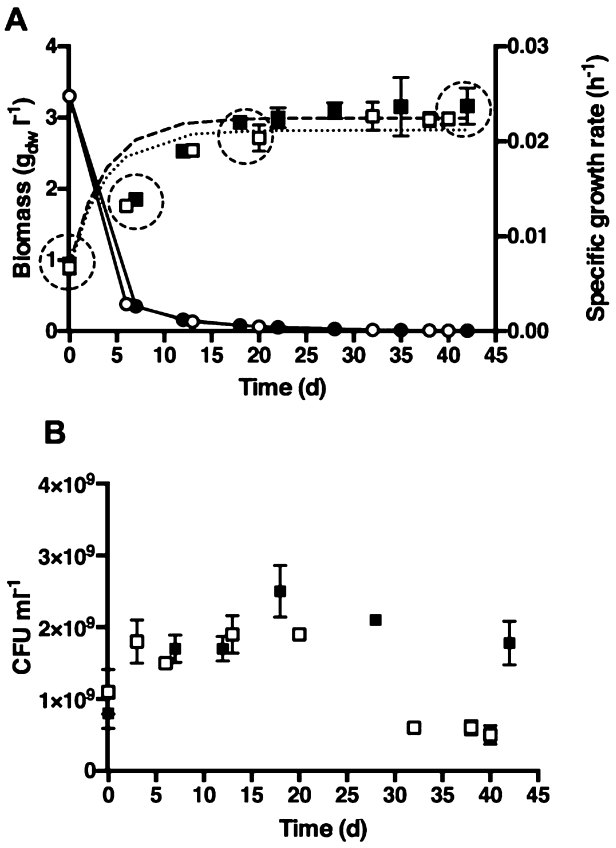

Fig. 2. Growth and viability of *B. subtilis* in retentostat cultures. Steady-state aerobic chemostat cultures (D = 0.025 h^{-1}) were switched to retentostat mode at time-point zero. Displayed are data from retentostat cultivation 1 (■) and 2 (□).
A. Measured biomass concentration (g_{dw} l^{-1}). Data points represent mean ± standard deviation of duplicate samples. Additionally, the biomass calculated with the fitted van Verseveld equation for retentostat 1 (—) and 2 (· · ·) is shown, as well as the corresponding calculated specific growth rates [(●) and (○) respectively]. Time-points analysed with transcriptomics are encircled for both retentostat cultivation 1 (0, 7, 18 and 42 days) and 2 (0, 6, 20 and 40 days). These encircled time-points are referred to as steady-state chemostats, time-points 1, time-points 2 and time-points 3.
B. Cultivability estimated by colony-forming units (CFU ml^{-1}) on solid medium. Data points represent mean ± standard deviation of triplicate samples.

[see *Materials and methods*, Eq. (5)] if the maintenance substrate requirement (m_s) and the maximum yield of biomass on the substrate (Y_{sx}^{max}) is independent of the specific growth rate (van Verseveld *et al.*, 1986). However, as Y_{sx}^{max} seems to be varying with the growth rate (see below), modelling with the van Verseveld equation will yield values different from measured values, which is indeed the case in the initial phase of retentostat culturing (Fig. 2A).

Next to the assumption of a constant m_s and Y_{sx}^{max}, two requirements are to be met for the van Verseveld equation: all biomass remains inside the bioreactor, and all biomass is viable and metabolically active (van Verseveld *et al.*, 1986). Both requirements are experimentally found to be met: Regular plating of effluent showed that no biomass escaped from the bioreactor and viability of the cultures was shown to be approximately 99% as assessed with fluorescence microscopy.

Colony-forming units (CFU), determined by plating of the culture, followed a trend during the first 20 days in correspondence with the biomass accumulation (Fig. 2B). Surprisingly, after approximately 20 days (between time-points 2 and 3) the CFU count decreased, while both the culture dry weight (Fig. 2A) and proportion of live cells (as detected by fluorescence analysis) remained stable. This was a decrease of approximately 30% for retentostat 1, and 70% for retentostat 2.

Cell morphology

Cell morphology was monitored using phase-contrast microscopy (Fig. 3A). In general, the cell morphology appeared to be heterogeneous. During the initial days of retentostat cultivation, cells were shaped like the typical *B. subtilis* rod with a few cells being shorter than normal. After roughly 20 days, when biomass accumulation reached a plateau and specific growth rates decreased to 0.0004 h^{-1}, a different cell morphology emerged. Cells that were longer than the typical rod started to appear, some reaching lengths of more than 10 times that of the usual vegetative single cell at the start of retentostat culturing. Additionally, most of these cells were bent or curved. The length of the cells and frequency of this aberrant morphology seemed to be proportional to the duration of retentostat culturing. In both retentostats these morphologies appeared, but to a greater extent in retentostat 2. The appearance of the elongated cells coincided with the observed decrease in CFU, with retentostat 2 having the most pronounced decrease in CFU and largest number of long cells. When a sample from the retentostat culture was grown overnight as batch in LB medium, microscopic examination showed that the elongated cells were no longer present and that solely the typical *B. subtilis* rod-shape could be observed.

In order to determine whether the elongated cells were single cells or composed of multiple undissociated cells, the cell membrane was visualized by incubating with the FM5-95 membrane dye (Invitrogen, UK). From microscopy images (Fig. 3B), it is clear that the filamentous cells are actually septated. Vigorous mixing did not lead to separation of the multiple compartments, confirming that the cells remained attached to each other. Additionally, the individual cells in such a chain appear to be elongated. When estimations of average cell number per chain in retentostat 2 were used to calculate the amount of CFU in a single cell and chained-cell scenario (results not

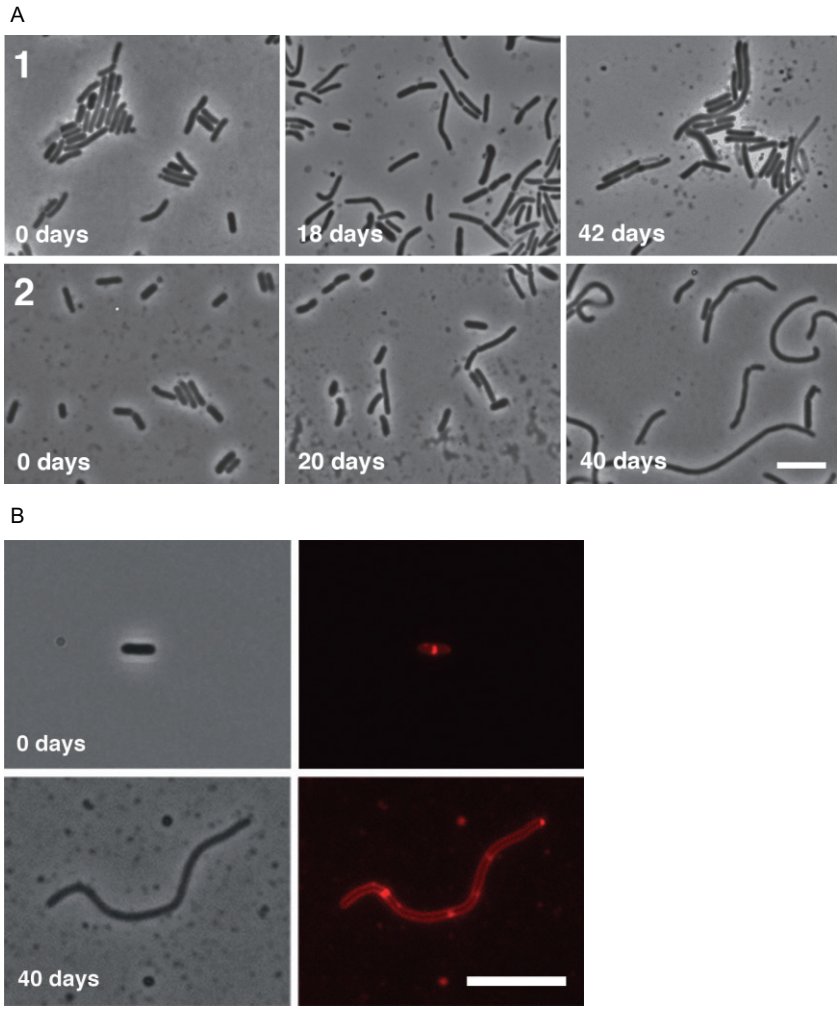

Fig. 3. A. Morphological changes of *B. subtilis* during retentostat cultivation. During a period of 42 and 40 days, an elongated morphology emerged in retentostat 1 and 2 respectively. First appearance of this morphology was after 18 and 20 days, respectively, coinciding with the biomass accumulation reaching a plateau. Scale bar indicates 5 μm. B. Membrane visualization in aberrant *B. subtilis* cells developed during retentostat cultivation. Staining of membranes with FM5-95 dye reveals that long cells are composed of multiple compartments. Shown are phase contrast and fluorescent microscopy images (left and right respectively). Scale bar indicates 5 μm.

shown), a decrease of 67% with chained cells was the outcome when compared with single cells. This calculated decrease is similar to the observed decrease in retentostat 2.

Maintenance coefficient and maximum growth yield

In a retentostat culture, progressive biomass accumulation leads to decreasing substrate availability per amount of biomass. When the substrate consumption rate (q_s) is plotted against time (Fig. 4A), it is visible that q_s approaches an asymptote: the value known as the maintenance substrate requirement (m_s; Pirt, 1965). Ultimately, when the point is reached where the q_s equals m_s, growth ceases. As is described in material and methods, q_s can be calculated from culture parameters.

If the maintenance substrate requirement and the yield of biomass on the substrate (Y_{sx}^{max}) are independent of the specific growth rate, they can be determined from the linear dependence of the glucose consumption rate over the whole range of specific growth rates achieved in the retentostat (Pirt, 1982; Boender *et al.*, 2009) (Fig. 4B). A linear trend line with an R^2 of 0.9605 and 0.9661 could be drawn through the data points of both retentostats. At a μ of zero, q_s equals m_s, which is the value at the Y-axis intercept. In the present study, m_s was found to be 0.24 mmol glucose g_{dw}^{-1} h^{-1}. The Y_{sx}^{max}, represented by 1/slope of the plot, turned out to be variable among different ranges of specific growth rates. The q_s from our steady-state chemostats at 0.025 h^{-1} was in agreement with data from higher growth rate chemostats (Dauner *et al.*, 2001), yielding a Y_{sx}^{max} of 64.56 mg_{dw} mmol $glucose^{-1}$. The average Y_{sx}^{max} over the range of growth rates in the current study (0.025 h^{-1} to 0.00006 h^{-1}) was determined to be 47.57 mg_{dw} mmol $glucose^{-1}$. At the lower growth rates, between 0.00275 h^{-1} and 0.00006 h^{-1}, a Y_{sx}^{max} of 16.74 mg_{dw} mmol $glucose^{-1}$ was found. Although there was a linear dependence of q_s over this lower range of growth rates, the variation found for the different ranges of growth rates indicates a variable Y_{sx}^{max}.

To be able to calculate the energy produced from glucose during retentostat culturing, residual glucose

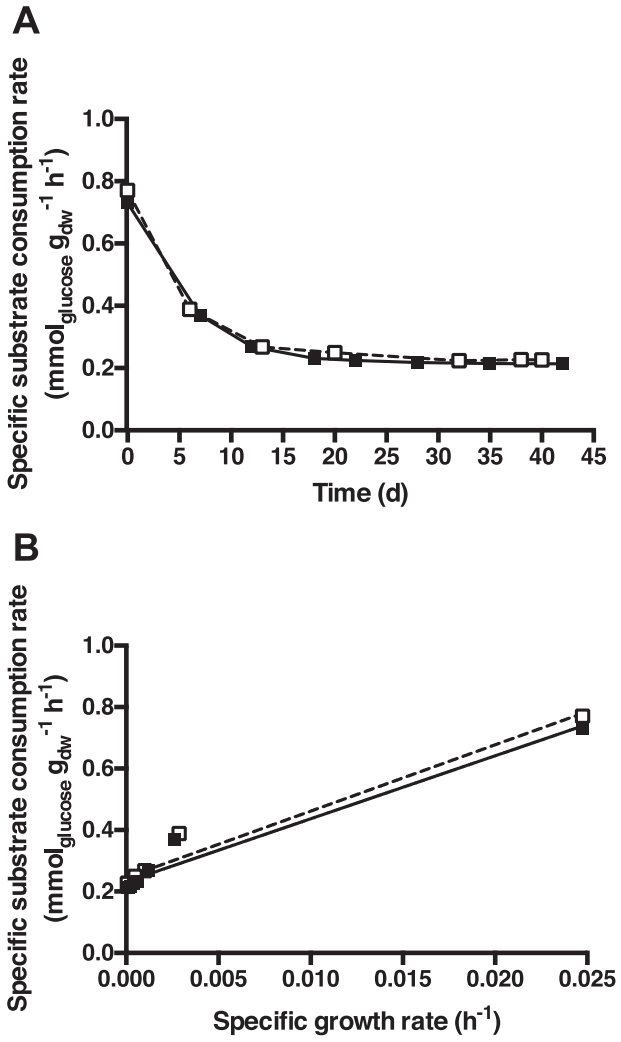

Fig. 4. Substrate consumption kinetics in retentostat cultures of *B. subtilis*. Steady-state aerobic chemostat cultures (D = 0.025 h^{-1}) were switched to retentostat mode at time-point zero. Displayed are data from retentostat cultivation 1 (■) and 2 (□).
A. Specific substrate consumption rate (q_s) asymptotically approaches the maintenance substrate requirement (m_s) during cultivation.
B. Relationship between specific substrate consumption rate (q_s) and specific growth rate (μ). Y-axis intersect of the plotted data determines the maintenance substrate requirement (m_s).

concentrations and catabolic end-products were determined by high-performance liquid chromatography (HPLC) analysis. The glucose concentration in the spent medium was below the detection limit. During retentostat cultivation, no metabolites were detected in the culture supernatant, indicating complete respiratory dissimilation of glucose. The amount of adenosine triphosphate (ATP) formed with dissimilation of glucose depends on the coupling efficiency of the electron transport chain to ATP synthesis. *Bacillus subtilis* possesses a three-branched electron transfer chain, of which the cytochrome *c* branch is inactive in glucose grown cells (Winstedt and von Wachenfeldt, 2000), and the *bd* oxidase branch is usually active under low oxygen conditions (Winstedt *et al.*, 1998). Most relevant for our cultures is the *aa3* oxidase branch, which is predominant in *B. subtilis* under oxygen-rich conditions (Winstedt and von Wachenfeldt, 2000). Transfer via this chain is expected to result in formation of 15 ATP per glucose molecule (Dauner *et al.*, 2001). Assuming that complete oxidation of a glucose molecule to carbon dioxide yields 15 ATP, the maintenance requirement for ATP (m_{atp}) is equivalent to 3.6 mmol ATP g_{dw}^{-1} h^{-1}.

The values for the maintenance energy coefficient m_s calculated above showed that during roughly 40 days of retentostat cultivation, the amount of substrate used for maintenance increased from approximately 30% at a growth rate of 0.025 h^{-1} to approximately 100% of the total substrate consumed at the end of the retentostat cultivation (see Fig. S1). The two independent retentostat cultures displayed highly similar growth kinetics, and the distribution of energy between maintenance and growth-related processes above shows that a near-zero growth state is reached during cultivation.

Transcriptome analysis of the retentostat cultures and overview of cellular processes regulated at the transcriptional level

Transcriptome analysis was performed at three time-points of the independent duplicate retentostat cultures, using chemostat-grown cells (μ = 0.025 h^{-1}) as a reference (Fig. 2). The multiple time-points during retentostat cultivation correspond to an increasing fraction of glucose used for maintenance purposes and hence to decreasing specific growth rates (Table 1).

Approximately, 12% of the genes were found to be differentially expressed at the end of retentostat cultivation; (gene expression rates of the individual retentostats can be found in Table 1). A total of 136 genes exhibited an increased relative messenger RNA (mRNA) level, whereas 377 genes exhibited a decreased relative mRNA level. A complete list of differentially expressed genes, including transcript ratios and statistical significance, has been deposited at Gene Expression Omnibus database (GEO; GSE55690).

The genes most prominently induced by zero-growth conditions in all time points are involved in glutamine uptake, fatty acid degradation and glucomannan uptake/utilization (Table S1). The most strongly repressed genes are involved in fructose uptake, mannitol uptake and methionine salvage (Table S1). Analysis of the transcriptome data on overrepresented functional categories in clusters of up- and downregulated genes revealed that transport and metabolism of carbohydrates, and of amino acids were enriched mostly among downregulated genes,

Table 1. Overview of gene regulation in retentostat conditions.

Time in retentostat (days)	Specific growth rate (h^{-1})	Percentage of initial growth rate (%)	Percentage of substrate used for maintenance (%)	Number of significantly regulated genes[a]		
				Total	Upregulated	Downregulated
Data from retentostat 1						
0	0.02475	100	31	N/A (reference condition)		
7	0.0026	11	56	97	31	66
18	0.0006	2.4	85	222	54	168
42	0.00006	0.24	98	236	46	190
Data from retentostat 2						
0	0.02475	100	31	N/A (reference condition)		
6	0.0028	11	57	65	54	11
20	0.0005	2	89	86	32	54
40	0.00006	0.24	98	339	169	170

a. significance criteria: $P < 0.05$; Fold-change > 2 or < –2.

but also among some upregulated genes (Fig. 5). Ribosomal and motility genes were prominent categories among the repressed genes, which also encompassed many genes encoding enzymes that are involved in glycolysis and biosynthesis of nucleotides, amino acids, fatty acids and cell wall components. This is in apparent agreement with reduced building block requirement in adaptation of the cells to the reduced substrate availability and decreased growth rate. Some genes involved in antibiotic production were upregulated.

Retentostat cultivation resulted in reduced expression of central glycolytic genes and relief of carbon catabolite repression

Although glucose starvation does not occur, a retentostat culture is consistently limited for glucose. The transcriptome analysis gives indications for tuning of energy-generating pathways to the reduced substrate access and growth. This is illustrated by repression of the CggR-regulated central glycolytic genes *gapA, pgk, pgm, eno* and *tpiA*.

Additionally, the transcriptome shows that adaptation to alternative-carbon-substrate utilization is occurring by relief of carbon catabolite repression (CCR). The CcpA-regulated genes *ctaDEF* and *qcrABC*, coding for cytochrome c oxidase *caa3* and for menaquinol: cytochrome c oxidoreductase (Liu and Taber, 1998; Blencke *et al*., 2003), respectively, are mildly upregulated. Together with induction of genes which are all repressed by CcpA in the presence of glucose such as *fadN* (fatty acid degradation) (Blencke *et al*., 2003; Tojo *et al*., 2011), *gmuB* (glucomannan utilization) (Sadaie *et al*., 2008) and *ara* genes (arabinose utilization) (Inácio *et al*., 2003), this suggests that CcpA repression is relieved under retentostat conditions (Fig. 5). Furthermore, there is relative lower abundance of *ilvB* operon transcripts, of which the production is positively controlled in the presence of glucose by interference of CcpA with CodY regulation (Shivers and Sonenshein, 2005).

Mild induction of the stringent response when specific growth rate decreases

About one third of the genes known to be under negative control of the stringent response by the pppGpp synthase RelA (Eymann *et al*., 2002; Bernhardt *et al*., 2003) are downregulated under retentostat conditions (Fig. 5). The observed downregulation increased in strength as the specific growth rate decreased. Many genes coding for components of the translational apparatus are found to be mildly downregulated. Among these genes are 26 ribosomal proteins, including the very large *rpsJ* operon and the initiation factor *infA*. Some genes, the products of which are involved in other processes typically associated with growing cells, are also found to be downregulated. A number of these are also known to be under RelA-dependent negative regulation (Eymann *et al*., 2002; Bernhardt *et al*., 2003), including genes functioning in RNA synthesis (*rpoA*), DNA replication (*dnaA*), nucleotide metabolism (*adk, pyrH*) and cell wall synthesis (*dltB, murA, murD*). The *secY* gene, coding for one of the Sec preprotein translocase subunits and known to be under stringent regulation (Eymann *et al*., 2002; Bernhardt *et al*., 2003) is downregulated, as well as genes functioning in energy metabolism such as the F_1F_0-ATPase encoding *atp* genes. In addition to the genes mentioned above, some growth-associated genes whose regulation is not dependent on RelA (Eymann *et al*., 2002) are also found to be downregulated under retentostat conditions (e.g. *pur* and *pyr* genes involved with nucleotide metabolism). Although many RelA-dependent genes were downregulated, none of the genes known to be induced during the stringent response (Eymann *et al*., 2002) were upregulated under retentostat conditions. Biosynthesis of branched chain

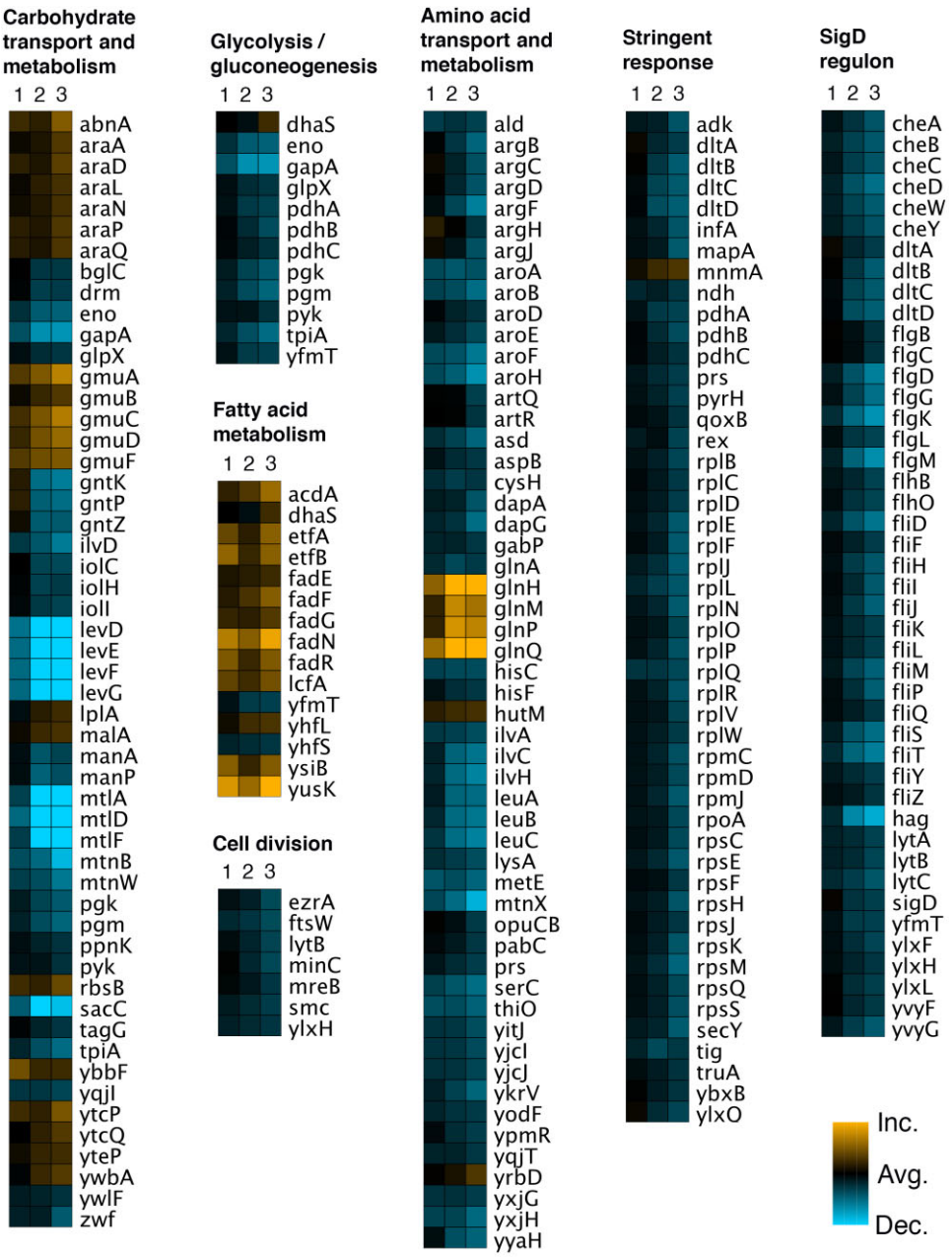

Fig. 5. Transcriptional adaptation to near-zero growth conditions. Displayed are the relative expression levels of each gene. The corresponding time-points are depicted above the columns. Comparisons are made with steady-state chemostat at $t = 0$. Colour indications are yellow for increased expression, blue for decreased expression and black for unchanged expression.

amino acids coded by the *ilv* operon was even found to be repressed at near-zero growth rates. In our retentostat cultures, a repression of CodY-regulated genes is observed.

There is no evidence to be found of σB-dependent general stress response (Hecker *et al*., 2007; Flórez *et al*., 2009) induction during retentostat cultivation when compared with chemostat conditions. No genes involved in the SOS response, which is activated upon DNA damage and other stresses that affect integrity of the genome (for a review see Lenhart *et al*., 2012), are induced. There are no indications for stationary phase mutagenesis as no repression of DNA repair systems such as the mismatch repair system (*mutSL*) and oxidized guanine (GO) system (*ytkD*, *mutM* and *yfhQ*) is observed (Pedraza-Reyes and Yasbin, 2004; Robleto *et al*., 2007; Vidales *et al*., 2009). Sporulation genes that are not *sigF* dependent [*spoIIE*, *spoIIGA*, *sigE* (*spoIIGB*) and *sigH*

(*spo0H*); Fawcett *et al*., 2000; Steil *et al*., 2005; Wang *et al*., 2006] are not induced.

Downregulation of motility and morphology-associated genes

The transcriptomics data show that many genes belonging to the σD regulon are downregulated in the retentostat sample (Fig. 5). Consistently, downregulation of the *sigD* gene and the activator of σD-dependent gene transcription, *swrB* (Kearns *et al*., 2004), was observed. Genes in the σD regulon code for proteins involved with flagella synthesis, chemotaxis and autolysis (Márquez *et al*., 1990). Most prominent among the downregulated σD-dependent genes are the large *flgB* operon and the *hag* gene, both involved in motility (Aizawa *et al*., 2002). Also found in this group is the operon *lytABC*, with *lytC* coding for a cell wall hydrolase (Blackman *et al*., 1998; Vollmer *et al*., 2008; Chen *et al*., 2009). This autolysin is mainly involved in motility and has a minor function in cell separation (Chen *et al*., 2009). Interestingly, there was a difference between the two retentostats in expression of two other cell wall hydrolases, *lytE* and *lytF*. These were downregulated only in retentostat 2 and 1 respectively. Both have an important function in cell separation because of their dexter-laevus (DL)-endopeptidase activity (Yamamoto *et al*., 2003; Fukushima *et al*., 2006). For localization to the cell wall, LytE interacts with the cytoskeletal protein MreBH (Carballido-López *et al*., 2006; Domínguez-Cuevas *et al*., 2013), of which the expression is downregulated in retentostat 2 only. Furthermore, the transcriptome revealed the repression in both retentostats of the genes *mreD* and *rodZ* which are part of the cell wall biosynthetic complex and involved in morphogenesis (Domínguez-Escobar *et al*., 2011; Garner *et al*., 2011; Muchová *et al*., 2013).

Induction of genes for antibiotics and secondary metabolites production

The *sigY* gene and the six other genes in the SigY regulon were upregulated under retentostat conditions. The sigma factor Y is found to be important for maintenance of the Sp-β prophage which contains genes necessary to produce and resist killing by the antibiotic sublancin (Mendez *et al*., 2012). The gene encoding the precursor of sublancin, *sunA*, is located on the Sp-β prophage (Paik *et al*., 1998) and was upregulated in our retentostat cultures.

Some genes coding for enzymes with industrial application were induced, including the alkaline protease encoding *aprE*, and the mannose-6-phosphate isomerase encoding *gmuF*. The latter is involved in glucomannan utilization by catalysing the conversion of among others L-ribulose to L-ribose, which is employed as a primary building block for the synthesis of various pharmaceutical compounds (Yeom *et al*., 2009).

Whole-genome re-sequencing

Sequencing of population samples revealed that in retentostat 1, a total of 60 single nucleotide polymorphisms (SNPs) were formed between day 18 and 42. Of these SNPs, 10 were in intergenic regions and 50 in coding regions. Of these 50 SNPs, 34 were determined to result in silent mutations. The remaining 16 resulted in missense mutations, affecting nine genes. None of the genes with SNPs in their upstream elements were differentially expressed in the transcriptome data. Additionally, 227 base pairs were deleted in the gene *ldh*. In retentostat 2, a total of eight SNPs were formed between day 20 and day 40, of which none were in intergenic regions. Of the total SNPs found, six were determined to be silent and two to result in missense mutations, affecting one gene. The majority of the mutations lie between 2 059 833 and 2 280 665 bp, known as the Sp-β prophage region (Lazarevic *et al*., 1999). For a list of SNPs resulting in missense mutations see Table S2. Similar to that of the population samples, the genomes of the single-colony isolates harboured SNPs almost exclusively in the Spβ prophage region (results not shown).

Discussion

The extremely low specific growth rate (0.0006 h^{-1}) reached at the end of the retentostat cultivation shows that cell retention is an effective way of reaching near-zero growth rates while maintaining a steady supply of nutrients. At this stage, all substrate consumed by the cells is used for maintenance purposes, which is estimated to be 0.24 mmol glucose g_{dw}^{-1} h^{-1}. The m_s was comparable to that found in studies on *B. subtilis* at higher growth rates (Sauer *et al*., 1996; Dauner and Sauer, 2001; Tännler *et al*., 2008). In these chemostat studies, the m_s was found to be ranging from 0.21 to 0.49 mmol glucose g_{dw}^{-1} h^{-1}.

Both Y_{sx}^{max} values found for steady-state chemostat (47.57 mg_{dw} mmol $glucose^{-1}$) and zero-growth retentostat cultures (16.74 mg_{dw} mmol $glucose^{-1}$) were lower than values determined in other chemostat studies that employed higher growth rates (between 67 and 82 ± 2 mg_{dw} mmol $glucose^{-1}$) (Sauer *et al*., 1996; Dauner *et al*., 2001; Tännler *et al*., 2008). The observed variability of the Y_{sx}^{max} value implies that the conversion of substrate to net biomass does not have a constant efficiency in *B. subtilis*. Various explanations may underlie these observations, including partial lysis of cells, or any other factor that results in higher biomass formation than is

measured, or specific growth-related processes that require elevated substrate consumption to generate the same biomass amount at low growth rates.

The progressively increasing number of (down)-regulated genes during the course of the retentostat cultivation indicates that transcriptional reprogramming took place to adapt the cellular physiology to limited carbon and energy availability. An example is the downregulation of *relA*-dependent genes, which suggests that the almost non-growing *B. subtilis* culture is subject to reduction of the translational apparatus by the stringent response in at least part of the culture (Eymann *et al*., 2002; Bernhardt *et al*., 2003). Furthermore, the repression of amino acid pathways, most likely by CodY (Molle *et al*., 2003), is a reflection of reduced building block requirement in non-growing cells. It is suggested that CodY plays a role in (p)ppGpp-mediated gene regulation: In stationary phase cells, genes regulated by the guanosine triphosphate (GTP)-binding protein CodY are de-repressed upon reduction of GTP levels. This can be due to conversion to (p)ppGpp or due to depletion of precursors necessary for guanine nucleotide synthesis (Geiger and Wolz, 2014). Repression of CodY-regulated genes observed in our retentostat cultures might suggest that GTP pools have remained at levels high enough to activate CodY repression. Biosynthetic pathway repression is illustrative for the fact that resources are diverted away from growth, parallel with the decreasing growth rates. This reaches a climax in extremely low growth rates and coincides with the strong redirection of substrate energy towards maintenance.

The decreased glucose consumption rate is reflected in the transcriptome as mild repression of central glycolytic genes, suggesting a fine tuning of glycolytic capacity in response to limited glucose availability. This repression is most likely due to low levels of fructose 1,6-bisphosphate (FBP) which consequently relieve the blockage on repression by CggR (Doan and Aymerich, 2003). In *B. subtilis*, carbon catabolism-related gene expression is regulated by FBP and glucose 6-phosphate-stimulated global regulator CcpA (Stülke and Hillen, 2000; Sonenshein, 2007). Reduced glycolytic capacity is known to result in a lower pool of HPrSer46P, which is a required co-regulator together with CcpA to mediate carbon catabolite repression (Stülke and Hillen, 2000). Although the residual glucose concentration in a glucose-limited chemostat is already very low, and CCR is expected to be relieved, the transcriptome indicates that CCR is even further relieved under retentostat conditions. As described by Monod kinetics, the glucose concentration drops further when the growth rate decreases (Monod, 1949; Senn *et al*., 1994), resulting in further relief of CCR under retentostat conditions. The consequential induction of genes involved in the utilization of alternative carbohydrates indicates that the adaptation of these cells to the severely limiting amounts of glucose leads to a prominent expansion of their active metabolic repertoire. At very low carbohydrate concentrations, the ability to simultaneously utilize various carbon sources, i.e. mixed substrate growth, most likely gives cells advantages over single substrate growth (Egli, 2010). Egli (2010) proposes 'improved metabolic/physiological flexibility' and 'improved kinetic performance', as cells growing in chemostats on mixed substrate were able to utilize the carbon sources at concentrations lower than observed in single-substrate chemostats (Lendenmann *et al*., 1996). Interestingly, the induction of genes involved in fatty acid degradation is described as essential for survival of non-growing *B. subtilis* cells by Koburger and colleagues (2005). Thus, the induction of fatty acid degradation genes in retentostat-cultivated cells potentially serves the goal of generating energy from an alternative source, e.g. phospholipids. There is no indication for lysis, but possibly membrane turnover could provide very low concentrations of fatty acids. The observed induction of fatty acid degradation genes is relatively strong and could indicate a more specific activation mechanism by fatty acids (Matsuoka *et al*., 2007) rather than solely CCR relief. Alternatively, this response could be an adaptation to expand the active metabolic repertoire, irrespective of the availability of the corresponding substrate, to be prepared for utilization once these metabolites occur in the environment.

The effects of reduced glucose availability are similar to those previously reported for batch culture cells experiencing glucose starvation upon transition to the stationary phase of growth (Koburger *et al*., 2005; de Jong *et al*., 2012). However, retentostat cultivation does prevent starvation by a continuous supply of glucose, which possibly explains the absence of reactions characteristic for stationary phase starvation such as the activation of the σB-dependent general stress response (Völker *et al*., 1995; Petersohn *et al*., 2001; Zhang and Haldenwang, 2005) and repression of DNA repair mechanisms characteristic for stationary phase mutagenesis (Robleto *et al*., 2007; Vidales *et al*., 2009). On the other hand, the σB general stress response, is only transiently activated (Völker *et al*., 1995; Holtmann *et al*., 2004), and this time window is possibly missed with the sample points taken.

Bacillus subtilis is a typical soil inhabitant, and while many soils provide limited amounts of carbon sources (Aldén *et al*., 2001; Ekblad and Nordgren, 2002; Ilstedt and Singh, 2005; Demoling *et al*., 2007), the maintenance metabolism does not seem to be specifically evolved for near-zero growth conditions under carbon limitation, because the maintenance coefficient calculated from retentostat cultivation and from extrapolated chemostat cultures at higher growth rates are virtually

identical. Instead, *B. subtilis* employs other strategies for survival under challenging conditions, such as the formation of endospores. The asporogenous *sigF* mutant used in this study is only able to express genes for sporulation initiation and thereby still allows us to see if sporulation is one of the responses *B. subtilis* applies. The fact that these genes are not differentially expressed under retentostat conditions in comparison with the chemostat reference condition, suggests that sporulation is not initiated under retentostat conditions. However, if sporulation is initiated under both retentostat and chemostat conditions, no differential expression would be observed as well. Sporulation has been previously reported in carbon-limited chemostats (Dawes and Mandelstam, 1970) and is regarded as a risk-spreading strategy (Fujita and Losick, 2005; Veening *et al*., 2008; de Jong *et al*., 2010), therefore it is very likely that sporulation is initiated under retentostat conditions.

The observed morphological heterogeneity and appearance of cell chains most likely is related to the regulation of the σD regulon. Expression of *sigD* is subject to stochasticity (Cozy and Kearns, 2010), and exponentially growing *B. subtilis* cultures are found to be heterogeneous in cell morphology, as they are epigenetically differentiated into two subpopulations with cells either ON or OFF for σD-dependent gene expression (Kearns and Losick, 2005; Chai *et al*., 2010). The former subpopulation grows as single motile cells, while the latter grows in non-motile chains. The decrease in the number of transcripts from σD-dependent genes in retentostat versus chemostat suggests that during retentostat cultivation, the proportion of cells that are ON for σD-dependent gene expression has decreased. The occurrence of the cell chains and elongation of cells (most prominent in retentostat 2) is likely correlated with the coinciding decline of CFU enumerations. Since the viability remained high and the culture dry weight did not decrease, it is unlikely that the decrease in CFUs is caused either by cell death or lysis. An alternative explanation for the observed decrease of the CFU count would be a change in the morphology of the cells, resulting in an increased weight per cell or chains of cells that form a single colony when plated, while actually representing multiple cells. Taking into account the average number of cells per chain enabled the accurate explanation of the reduced CFU numbers, indicating that chain formation is the predominant explanation for the observed CFU decline. The retentostat-adapted cell chains rapidly reverted to the typical *B. subtilis* rod shape when inoculated in normal batch culture conditions, illustrating that this condition-dependent morphology is a response to retentostat cultivation. The repression of genes coding for autolysins (*lytC, lytE and lytF*) and other members of the cell wall biosynthetic complex (*mreBH*, *mreD*, *rodZ*) are possibly the direct cause of the changed morphology under retentostat conditions (Ishikawa *et al*., 1998; Carballido-López *et al*., 2006; Chen *et al*., 2009). The observed curved long-chained morphology is very similar to that of *lytE* (Ishikawa *et al*., 1998) and *lytF* mutants (Ohnishi *et al*., 1999; Chen *et al*., 2009). Mutation of these cell wall hydrolase-encoding genes prevents the appropriate rate of digestion of peptidoglycan strands, which is a prerequisite for normal cell separation, and thereby results in long cell chains. It has been suggested that *lytE* and *lytF* have overlapping functions here (Ishikawa *et al*., 1998; Ohnishi *et al*., 1999; Carballido-López *et al*., 2006). Downregulation of *lytE* and *lytF* in retentostat 2 and 1, respectively, is therefore likely to have contributed to the chained-cell morphology, whereas the higher number of cell-chains in retentostat 2 may be related to the observed co-repression of *mreBH* in this culture, next to the *lytE* repression. The cytoskeletal protein MreBH is responsible for localization of LytE to the lateral cell wall, and *mreBH* mutants have a curved long-chained morphology very similar to that observed in this study (Carballido-López *et al*., 2006). Based on these findings, we propose that the observed morphology is caused by the repression of the specific functions in cell wall metabolism, and that the magnitude of the morphological effect may relate to the degree of repression of particular subsets of these functions. The few slightly shorter cells observed mainly in the beginning of retentostat culturing seem similar to phenomena observed in *E. coli* such as dwarfing or reductive cell division (Nyström, 2004b). Both processes occur in stationary phase and result in size reduction. Whether the shorter cells under retentostat conditions are indeed a result of these phenomena remains to be elucidated.

Growth-related genome mutation rates are proportional to the number of DNA replications within a growing culture (Drake, 1991; Drake *et al*., 1998; Barrick *et al*., 2009). Because only approximately four generations are formed during the course of 40-day retentostat cultivation as estimated from specific growth rates, these mutations most likely are not very numerous. However, lysis of cells and regrowth of others at the same rate (cryptic growth; Ryan, 1959; Finkel, 2006) could lead to higher growth rates than estimated. As growth is a requirement for propagation of genetic variants throughout a population (Berg *et al*., 2002; Finkel, 2006), the number of mutations in the genome could reveal whether substantial growth has taken place or not. A low number of SNPs, almost entirely confined to the SP-beta prophage region, confirm that limited cryptic growth has taken place in the retentostat. The Sp-beta prophage is known as a region where deletions occur, sometimes at high frequency (Spancake and Hemphill, 1985). This suggests it is dispensible, as shown by Westers and colleagues (2003).

This work shows that retentostat culturing is (apart from some pitfalls mentioned above) a controlled and stable cultivation condition, suitable for the study of extremely slow growing cultures of *B. subtilis*, which allocate the vast majority of substrate derived energy to maintenance. Our study reveals that retentostat cultivation has many characteristics in common with stationary-phase cultures, but also several fundamental differences are apparent. High-cell viability and no significant induction of systems involved with DNA and protein repair, indicate that deterioration of cellular functions as observed in stationary phase is absent in retentostat cultures. Moreover, lack of mismatch repair repression, characteristic for stationary phase mutagenesis, together with a low number of SNPs, underpins the difference between retentostat cells and stationary phase cells and confirms that retentostat cultivation provides a method to achieve extremely slow growth rates without the loss of cell integrity and function.

Experimental procedures

Strain, growth conditions and media

Bacillus subtilis 168 *trpC2 sigF::spec amyE::*P_{rrnB}*-gfp* + was used for the retentostat experiments in this study. This strain carries a GFP fusion to the promoter of the constitutively expressed ribosomal RNA operon *rrnB* (Krásný and Gourse, 2004; Veening *et al.*, 2009), and is defective in sporulation, caused by a disruption in the *sigF* gene. Pre-cultures for chemostat and retentostat cultivations were prepared by inoculating a single colony from an lysogeny broth (LB) agar plate into 10 ml LB medium (Sambrook *et al.*, 1989). This culture was grown at 37°C until an optical density at 600 nm (OD_{600}) of 0.3 was reached. Subsequently, 1000x dilutions were made in 60 ml M9 medium (Miller, 1972) supplemented with 27.75mM glucose and 0.1mM Tryptophan. The M9 minimal medium contained, per litre of deionized water, 8.5 g of $Na_2HPO_4 \cdot 2H_2O$, 3.0 g of KH_2PO_4, 1 g of NH_4Cl and 0.5 g of NaCl. The following components were sterilized separately and added per litre: 1 ml of 0.1 M $CaCl_2$, 1 ml of 1 M $MgSO_4$, 1 ml of 50 mM $FeCl_3$ and 10 ml of M9 trace salts solution. The M9 trace salts solution contained (per litre) 0.1 g $MnCl_2 \cdot 4H_2O$, 0.17 g of $ZnCl_2$, 0.043 $CuCl_2 \cdot 2H_2O$, 0.06 $CoCl_2 \cdot 6H_2O$, 0.06 $Na_2MoO_4 \cdot 2H_2O$. The cultures were grown overnight and used for inoculation of the bioreactors. Chemostat and retentostat media were acidified to pH 5 by addition of H_2SO_4 (95 to 97%) to avoid precipitation of medium components. During the cultivation in the bioreactors, the pH was maintained at 7.0 by automatic addition of NaOH 5M.

Chemostat cultivation

Duplicate chemostat cultures were performed at a dilution rate, D [defined as the ratio of the medium feed rate (l h^{-1}) and culture volume (l)] of 0.025 h^{-1}. 2.0 l bioreactors (Infors Benelux BV, the Netherlands) with 1.4 l working volume were inoculated with an exponentially growing pre-culture to start the chemostats. The bioreactors were operated at 37°C under aerobic conditions. An airflow of 0.1 l min^{-1} and a stirring speed of 800 r.p.m. was set to keep oxygen levels above 50% of air-saturation.

The working volume was kept constant by means of a conductivity sensor placed at the surface of the culture, activating a peristaltic pump that removed effluent. To prevent foam formation, 5 ml of a 5% (wt.wt^{-1}) solution of the antifoaming agent Struktol J673 (Schill and Seilacher AG, Hamburg, Germany) was added per 24 h, automatically spread over intervals of 13 min. Steady state was defined as the condition in which culture parameters were constant for at least five volume changes and when optical density at 600 nm (OD_{600}) and cell dry weight had remained constant (< 5% and < 10% variation, respectively) for at least two volume changes. Culture purity was routinely checked by phase-contrast and fluorescence microscopy. The P*rrnB*–GFP fusion allowed for identification of fluorescent cells as being the inoculated *B. subtilis*. Additionally, cells were plated on LB agar plates to check for possible contaminations.

Retentostat cultivation

A 2.0 L bioreactor (Infors Benelux BV, the Netherlands) was equipped with an autoclavable polyethersulfone cross-flow filter with a pore size of 0.22 μm (Spectrum Laboratories, CA, USA) to retain biomass in the reactor. The filter was connected to the bioreactor via an external loop, through which culture was circulated.

Two individual retentostat experiments were initiated from chemostat cultures at dilution rates of 0.025 h^{-1}. After reaching steady state in the chemostat, the bioreactors were switched to retentostat mode by withdrawing the effluent through the filter instead of through the standard effluent tube. The retentostat cultivations were operated under the same conditions (temperature, pH, medium flow rate, oxygenation, stirring rate, anti-foam addition) as the chemostats. Since withdrawal of biomass from the culture influences the kinetics of biomass accumulation, sampling volumes and frequency were kept to a minimum. The super safe sampler ports (Infors Benelux BV, the Netherlands) that were used for fast and aseptic sample withdrawal, allowed for accurate control of the sample volume.

Determination of biomass, substrate and metabolites

During chemostat and retentostat cultivation, samples were withdrawn from the bioreactor to determine biomass, glucose and organic acid concentrations. Cell dry weight was determined in duplicate by cooled centrifugation of 5 ml of culture in pre-weighted tubes, washing with 0.9% NaCl and drying at 105°C for 24 h to constant weight. Additionally, the optical density of the culture was determined by measuring the optical density at 600 nm. Glucose and organic acid concentrations in culture supernatants were determined by HPLC (Shimadzu Scientific Instruments, MD, USA), using LC SOLUTIONS SP1 software from Shimadzu (Kyoto, Japan). Culture supernatants were obtained by centrifugation (10 000 g for 10 min at 4°C), filter sterilized and stored at –20°C until HPLC analysis. Samples were separated using an Aminex HPX-87H anion-exchange column (Bio-rad Laboratories, Rich-

mond, CA) with sulfuric acid (5 mM; 0.6 ml min^{-1}) as mobile phase at 55°C. Detection was performed with a refractive index detector and UV wavelength absorbance detector (Shimadzu Scientific Instruments, MD, USA).

Assessment of cell viability

To estimate the fraction of dead cells in culture samples, the red fluorescent compound propidium iodide (PI) was used. Propidium iodide binds DNA and can only do so in cells with permeabilized membranes. A 10 μL culture sample was washed and re-suspended in 990 μL 0.85% NaCl and 1 μL of PI (20 mM dissolved in dimethylsulphoxide) was added and incubated for 10 min. The P*rrnB*–GFP fusion this strain carries causes metabolically active cells to produce GFP, and these could thus be detected as alive. Enumeration of live and dead cell fractions was performed using these PI and GFP markers, in a Deltavision (Applied Precision) IX7 1DV Microscope (Olympus) which is described in more detail below. Additionally, CFU quantification was performed by plating 10-fold dilution series of the cultures (five to seven dilutions in LB broth) in triplicate on LB agar (1.5% wt/vol) plates. After 24 h of incubation at 37°C, colonies were counted.

Microscopy and analysis of cell morphology

Cell morphology was analysed by phase-contrast and fluorescence microscopy. In order to visualize the cell membrane, cells were incubated for 1 min with an ice-cold 5 μg/ml FM5-95 membrane dye solution (Invitrogen, UK) prior to microscopy analysis. Images were taken with Deltavision (Applied Precision) IX71Microscope (Olympus) using a CoolSNAP HQ2 camera (Princeton Instruments) with a 100 × phase-contrast objective. Fluorescence filter sets used to visualize GFP (excitation at 450/90 nm; emission at 500/50 nm) and red dyes (excitation at 572/35 nm, emission 632/60 nm) were from Chroma Technology Corporation (Bellows Falls, USA). Exposure time was between 0.2 and 1 s with 32% transmission xenon light (300 W). Exposure time for phase-contrast images was 0.05 s. SOFTWORX 3.6.0 (Applied Precision) software was used for image capturing. Time-lapse microscopy was performed as described before (de Jong *et al.*, 2011).

Calculation of retentostat growth kinetics

The following mass balance equations are used to calculate growth kinetics in retentostat cultivations. Equation 1 is for biomass, assuming complete cell retention and constant volume. Equation 2 is for substrate. Here, C_x is the biomass concentration (g l^{-1}), μ is the specific growth rate (h^{-1}), C_s is the residual glucose concentration (g l^{-1}), D is the dilution rate (h^{-1}), $C_{s,in}$ is the glucose concentration in the feed (g l^{-1}) and q_s is the specific glucose consumption rate (g g^{-1} h^{-1}).

$$\frac{dC_x}{dt} = \mu \cdot C_x \tag{1}$$

$$\frac{dC_s}{dt} = D(C_{s,in} - C_s) - q_s \cdot C_x \tag{2}$$

With the assumptions that variation of the glucose concentration in the bioreactor is negligible in comparison to the amount of glucose supplied with fresh medium ($dC_s/dt \ll D\,C_{s,in}$) and that the residual glucose concentration in the broth (consistently below the detection limit) is much smaller than the glucose concentration in the medium, q_s can be calculated with Eq. (3).

$$q_s = \frac{D \cdot C_{s,in}}{C_x} \tag{3}$$

The Herbert–Pirt (Pirt, 1982) equation (Eq. 4) describes the relation between specific substrate consumption rate (q_s), specific growth rate (μ), maximum biomass yield on substrate (Y_{sx}^{max}) and maintenance energy coefficient (m_s).

$$q_s = \frac{\mu}{Y_{sx}^{max}} + m_s \tag{4}$$

Equation 4 was used to determine m_s and Y_{sx}^{max}. This was done by plotting the values of q_s against μ. The intercept of a linear regression line with the y-axis determines m_s. Y_{sx}^{max} was calculated by taking the slope^{-1} of the regression line.

The biomass accumulation during retentostat cultivation can be described by the van Verseveld equation (van Verseveld *et al.*, 1986) (Eq. 5).

$$C_x(t) = \left(C_{x,0} - \frac{D(C_{s,in} - C_s}{m_s}\right) \cdot e^{-m_s \cdot Y_{sx}^{max} \cdot t} + \frac{D(C_{s,in} - C_s)}{m_s} \tag{5}$$

This equation assumes an ideal situation with no loss of viability and growth rate independent maintenance-energy requirements.

The specific growth rate of the retentostat cultivations is calculated with Eq. (6):

$$\mu = \frac{dC_{x,total}/dt}{c_{x,viable}} \tag{6}$$

In order to determine the derivative of the biomass accumulation data ($dC_{x,total}/dt$), the measured total biomass concentrations (viable and non-viable cells) were fitted with the equation $C_x = A \cdot e^{B \cdot t} + C$, which is of the same shape as Eq. (5). This was done using GRAPHPAD PRISM 6 (GraphPad Software Inc., USA), minimizing the sum of squares of errors by varying *A, B* and *C*. With *A, B* and *C* known, the derivative ($dC_{x,total}/dt$) could be determined. Because only viable biomass can replicate, this is incorporated in the equation. The doubling time of the culture is calculated by dividing the natural logarithm of 2 by the specific growth rate.

DNA microarray experiments and analysis

Transcriptome analysis on four time points of independent duplicate retentostat cultures was performed as follows. For RNA isolation, cell culture samples were quickly centrifuged for 2 min at 6000 × g, and frozen in liquid nitrogen. Cells were broken using 500 mg of glass beads, 500 μl of phenol-chloroform, 30 μl of 3 M sodium acetate and 15 μl of 20% sodium dodecyl sulfate. Ribonucleic acids were isolated using the High Pure RNA isolation kit (Roche, Mannheim, Germany) according to the manufacturer's instructions. After a quality check of the isolated RNA using an Agilent Bioanalyzer 2100 with RNA 6000 LabChips (Agilent

Technologies, the Netherlands), 20 μg of total RNA was used for complementary DNA (cDNA) synthesis and incorporation of aminoallyl-dUTP using SuperscriptIII reverse transcriptase (Invitrogen, Life Technologies Europe BV, the Netherlands). Subsequently, the cDNA was labeled with Dylight 550 or Dylight 650 Dyes (Thermo Scientific Pierce, Rockford, USA) as described before (van Hijum *et al*., 2005; Lulko *et al*., 2007). Hybridization was performed on *B. subtilis* 168 Agilent 8x15k DNA microarrays (GEO platform GPL18393) at 65°C as described in the Agilent Two-Color microarray manual (v1.3). These slides contained two to three probes of each gene. For hybridization, the following cDNA comparisons were made: (i) chemostats with the retentostat time-points 1 (indicated in Fig. 2), (ii) time-points 1 with time-points 2, (iii) time-points 2 with time-points 3, (iv) time-points 3 with chemostats, (v) chemostats with time-points 2, (vi) time-points 1 with time-points 3. This resulted in a total of 24 slides used for this study. Slides were scanned using a confocal laser scanner (GenePix Autoloader AL4200, Molecular Devices, Sunnyvale, USA). Fluorescent signal intensity data were quantified using GenePix 6.1 (Molecular Devices Ltd., Sunnyvale, USA). The data sets were Lowess normalized, and a statistical analysis was performed using the LimmaR software package (Smyth, 2004). Following the Limma R pipeline, the multiple values of genes with a multi-probe design are merged to one value by taking the average ln(ratio) and the $e^{(\text{average ln(p-values)})}$. Genes showing a fold change higher then 1.5 and a Benjamini Hochberg corrected *P* value (Benjamini and Hochberg, 1995) of < 0.05 were considered to be significantly altered in expression. Functional analysis on http://server.molgenrug.nl was used to calculate which functional classes were overrepresented in the DNA microarray data for each of the time-points. Various annotation sources were used in this enrichment analysis: metabolic pathways from Kyoto Encyclopedia of Genes and Genomes (KEGG; Kanehisa *et al*., 2004), categories from Gene Ontology (GO; Ashburner *et al*., 2000) and Cluster of Orthologous Groups (Tatusov *et al*., 1997) and regulons from Database of Transcriptional regulation in *B. subtilis* (Sierro *et al*., 2008).

The microarray data have been deposited in the GEO database (http://ncbi.nlm.nih.gov/geo/) under the accession number GSE55690.

Whole-genome sequencing

In order to re-sequence the genome of retentostat grown cells, genomic DNA was isolated by phenol/chloroform extraction using Phase Lock Gel Heavy 2 ml tubes (5 PRIME, Hilden, Germany). The full genomes of the following population samples were sequenced: (i) the strain used for the initial inoculum; (ii) retentostats at time-point 2; and (iii) the end-point of both retentostat cultures at time-point 3 (see Fig. 2). In addition, the genomes of two single colony isolates of retentostat culture 1 at time-point 3 were sequenced. Genome sequencing was performed using paired-end sequencing with 100 bp runs on an Illumina HiSeq 2000 using a library of 500 bp fragments. Data from the genome sequencing was analysed with the breseq software pipeline using default settings (Barrick *et al*., 2009). Single nucleotide polymorphisms and insertions/deletions (indel) of retentostat strains were identified by comparison with the strain used for inoculation.

Acknowledgements

We thank Bert van der Bunt, Marjo Starrenburg and Erik de Hulster for valuable help with the bioreactors; Mark Bisschops for valuable help with calculations; Agata Pudlik and Tim Vos for valuable help with HPLC analysis; Anne de Jong for valuable help with micro-array analysis; members of the joint zero-growth project group (Kluyver Centre, the Netherlands) for support and valuable discussions; and Sietse Koenders for the illustration in Fig. 1.

This work was carried out within the research programme of the Kluyver Centre for Genomics of Industrial Fermentation which is part of the Netherlands Genomics Initiative/Netherlands Organization for Scientific Research.

Conflict of interest

The authors declare that they have no conflict of interest.

References

Aizawa, S., Zhulin, I.B., Márquez-Magaña, L., and Ordal, G.W. (2002) Chemotaxis and motility. In *Bacillus Subtilis and Its Closest Relative: From Genes to Cells*. Sonenshein, A.L., Hoch, J.A., and Losick, R. (eds). Washington, DC, USA: ASM Press, pp. 437–452.

Aldén, L., Demoling, F., and Bååth, E. (2001) Rapid method of determining factors limiting bacterial growth in soil. *Appl Environ Microbiol* **67:** 1830–1838.

Arbige, M., and Chesbro, W.R. (1982) Very slow growth of *Bacillus polymyxa*: stringent response and maintenance energy. *Arch Microbiol* **132:** 338–344.

Ashburner, M., Ball, C.A., Blake, J.A., Botstein, D., Butler, H., Cherry, J.M., *et al*. (2000) Gene ontology: tool for the unification of biology. The gene ontology consortium. *Nat Genet* **25:** 25–29.

Barrick, J.E., Yu, D.S., Yoon, S.H., Jeong, H., Oh, T.K., Schneider, D., *et al*. (2009) Genome evolution and adaptation in a long-term experiment with *Escherichia coli*. *Nature* **461:** 1243–1247.

Benjamini, Y., and Hochberg, Y. (1995) Controlling the false discovery rate: a practical and powerful approach to multiple testing. *J R Stat Soc Series B Stat Methodol* **57:** 289–300.

Berg, J.M., Tymoczko, J.L., and Stryer, L. (2002) *Biochemistry*, Fifth edn. New York: W.H. Freeman.

Bernhardt, J., Weibezahn, J., Scharf, C., and Hecker, M. (2003) *Bacillus subtilis* during feast and famine: visualization of the overall regulation of protein synthesis during glucose starvation by proteome analysis. *Genome Res* **13:** 224–237.

Blackman, S.A., Smith, T.J., and Foster, S.J. (1998) The role of autolysins during vegetative growth of *Bacillus subtilis* 168. *Microbiology* **144** (Part 1): 73–82.

Blencke, H.-M., Homuth, G., Ludwig, H., Mäder, U., Hecker, M., and Stülke, J. (2003) Transcriptional profiling of gene expression in response to glucose in *Bacillus subtilis*: regulation of the central metabolic pathways. *Metab Eng* **5:** 133–149.

Blom, E.-J., Ridder, A.N.J.A., Lulko, A.T., Roerdink, J.B.T.M., and Kuipers, O.P. (2011) Time-resolved transcriptomics

and bioinformatic analyses reveal intrinsic stress responses during batch culture of *Bacillus subtilis*. *PLoS ONE* **6:** e27160.

van Bodegom, P. (2007) Microbial maintenance: a critical review on its quantification. *Microb Ecol* **53:** 513–523.

Boender, L.G.M., de Hulster, E.A.F., van Maris, A.J.A., Daran-Lapujade, P.A.S., and Pronk, J.T. (2009) Quantitative physiology of *Saccharomyces cerevisiae* at near-zero specific growth rates. *Appl Environ Microbiol* **75:** 5607–5614.

Branda, S.S., González-Pastor, J.E., Ben-Yehuda, S., Losick, R., and Kolter, R. (2001) Fruiting body formation by *Bacillus subtilis*. *Proc Natl Acad Sci USA* **98:** 11621–11626.

Brock, T.D. (1971) Microbial growth rates in nature. *Bacteriol Rev* **35:** 39–58.

Carballido-López, R., Formstone, A., Li, Y., Ehrlich, S.D., Noirot, P., and Errington, J. (2006) Actin homolog MreBH governs cell morphogenesis by localization of the cell wall hydrolase LytE. *Dev Cell* **11:** 399–409.

Chai, Y., Norman, T., Kolter, R., and Losick, R. (2010) An epigenetic switch governing daughter cell separation in *Bacillus Subtilis*. *Genes Dev* **24:** 754–765.

Chen, R., Guttenplan, S.B., Blair, K.M., and Kearns, D.B. (2009) Role of the sigmaD-dependent autolysins in *Bacillus subtilis* population heterogeneity. *J Bacteriol* **191:** 5775–5784.

Chesbro, W., Evans, T., and Eifert, R. (1979) Very slow growth of *Escherichia coli*. *J Bacteriol* **139:** 625–638.

Cozy, L.M., and Kearns, D.B. (2010) Gene position in a long operon governs motility development in *Bacillus subtilis*. *Mol Microbiol* **76:** 273–285.

Daran-Lapujade, P., Daran, J.-M., van Maris, A.J.A., de Winde, J.H., and Pronk, J.T. (2009) Chemostat-based micro-array analysis in baker's yeast. *Adv Microb Physiol* **54:** 257–311.

Dauner, M., and Sauer, U. (2001) Stoichiometric growth model for riboflavin-producing *Bacillus subtilis*. *Biotechnol Bioeng* **76:** 132–143.

Dauner, M., Storni, T., and Sauer, U. (2001) *Bacillus subtilis* metabolism and energetics in carbon-limited and excess-carbon chemostat culture. *J Bacteriol* **183:** 7308–7317.

Dawes, I.W., and Mandelstam, J. (1970) Sporulation of *Bacillus subtilis* in continuous culture. *J Bacteriol* **103:** 529.

Demoling, F., Figueroa, D., and Bååth, E. (2007) Comparison of factors limiting bacterial growth in different soils. *Soil Biol Biochem* **39:** 2485–2495.

Doan, T., and Aymerich, S. (2003) Regulation of the central glycolytic genes in *Bacillus subtilis*: binding of the repressor CggR to its single DNA target sequence is modulated by fructose-1,6-bisphosphate. *Mol Microbiol* **47:** 1709–1721.

Domínguez-Cuevas, P., Porcelli, I., Daniel, R.A., and Errington, J. (2013) Differentiated roles for MreB-actin isologues and autolytic enzymes in *Bacillus subtilis* morphogenesis. *Mol Microbiol* **89:** 1084–1098.

Domínguez-Escobar, J., Chastanet, A., Crevenna, A.H., Fromion, V., Wedlich-Söldner, R., and Carballido-López, R. (2011) Processive movement of MreB-associated cell wall biosynthetic complexes in bacteria. *Science* **333:** 225–228.

Drake, J.W. (1991) A constant rate of spontaneous mutation in DNA-based microbes. *Proc Natl Acad Sci USA* **88:** 7160–7164.

Drake, J.W., Charlesworth, B., Charlesworth, D., and Crow, J.F. (1998) Rates of spontaneous mutation. *Genetics* **148:** 1667–1686.

Dubnau, D. (1991) Genetic competence in *Bacillus subtilis*. *Microbiol Rev* **55:** 395–424.

Dworkin, J., and Losick, R. (2005) Developmental commitment in a bacterium. *Cell* **121:** 401–409.

Egli, T. (2010) How to live at very low substrate concentration. *Water Res* **44:** 4826–4837.

Ekblad, A., and Nordgren, A. (2002) Is growth of soil microorganisms in boreal forests limited by carbon or nitrogen availability? *Plant Soil* **242:** 115–122.

Ercan, O., Smid, E.J., and Kleerebezem, M. (2013) Quantitative physiology of *Lactococcus lactis* at extreme low-growth rates. *Environ Microbiol* **15:** 2319–2332.

Errington, J. (2003) Regulation of endospore formation in *Bacillus subtilis*. *Nat Rev Microbiol* **1:** 117–126.

Eymann, C., Homuth, G., Scharf, C., and Hecker, M. (2002) *Bacillus subtilis* functional genomics: global characterization of the stringent response by proteome and transcriptome analysis. *J Bacteriol* **184:** 2500–2520.

Fawcett, P., Eichenberger, P., Losick, R., and Youngman, P. (2000) The transcriptional profile of early to middle sporulation in *Bacillus subtilis*. *Proc Natl Acad Sci USA* **97:** 8063–8068.

Ferenci, T. (2001) Hungry bacteria – definition and properties of a nutritional state. *Environ Microbiol* **3:** 605–611.

Finkel, S.E. (2006) Long-term survival during stationary phase: evolution and the GASP phenotype. *Nat Rev Microbiol* **4:** 113–120.

Flórez, L.A., Roppel, S.F., Schmeisky, A.G., Lammers, C.R., and Stülke, J. (2009) A community-curated consensual annotation that is continuously updated: the *Bacillus subtilis* centred wiki SubtiWiki. *Database (Oxford)* **2009:** bap012.

Fujita, M., and Losick, R. (2005) Evidence that entry into sporulation in *Bacillus subtilis* is governed by a gradual increase in the level and activity of the master regulator Spo0A. *Genes Dev* **19:** 2236–2244.

Fukushima, T., Afkham, A., Kurosawa, S.-I., Tanabe, T., Yamamoto, H., and Sekiguchi, J. (2006) A new D,L-endopeptidase gene product, YojL (renamed CwlS), plays a role in cell separation with LytE and LytF in *Bacillus subtilis*. *J Bacteriol* **188:** 5541–5550.

Garner, E.C., Bernard, R., Wang, W., Zhuang, X., Rudner, D.Z., and Mitchison, T. (2011) Coupled, circumferential motions of the cell wall synthesis machinery and MreB filaments in *B. subtilis*. *Science* **333:** 222–225.

Geiger, T., and Wolz, C. (2014) Intersection of the stringent response and the CodY regulon in low GC Gram-positive bacteria. *Int J Med Microbiol* **304:** 150–155.

Goffin, P., van de Bunt, B., Giovane, M., Leveau, J.H.J., Höppener-Ogawa, S., Teusink, B., and Hugenholtz, J. (2010) Understanding the physiology of *Lactobacillus plantarum* at zero growth. *Mol Syst Biol* **6:** 413.

Hecker, M., Pané-Farré, J., and Völker, U. (2007) SigB-dependent general stress response in *Bacillus subtilis* and related gram-positive bacteria. *Annu Rev Microbiol* **61:** 215–236.

Herbert, D. (1961) A theoretical analysis of continuous culture systems. In *Continuous Culture of Micro-Organisms*. London, UK: Society of Chemical Industry, pp. 21–53.

Herbert, D., Elsworth, R., and Telling, R.C. (1956) The continuous culture of bacteria: a theoretical and experimental study. *J Gen Microbiol* **14:** 601–622.

van Hijum, S.A.F.T., de Jong, A., Baerends, R.J.S., Karsens, H.A., Kramer, N.E., Larsen, R., *et al*. (2005) A generally applicable validation scheme for the assessment of factors involved in reproducibility and quality of DNA-microarray data. *BMC Genomics* **6:** 77.

Holtmann, G., Brigulla, M., Steil, L., Schutz, A., Barnekow, K., Volker, U., and Bremer, E. (2004) RsbV-independent induction of the SigB-dependent general stress regulon of *Bacillus subtilis* during growth at high temperature. *J Bacteriol* **186:** 6150–6158.

Ilstedt, U., and Singh, S. (2005) Nitrogen and phosphorus limitations of microbial respiration in a tropical phosphorus-fixing acrisol (ultisol) compared with organic compost. *Soil Biol Biochem* **37:** 1407–1410.

Inácio, J.M., Costa, C., and de Sá-Nogueira, I. (2003) Distinct molecular mechanisms involved in carbon catabolite repression of the arabinose regulon in *Bacillus subtilis*. *Microbiology* **149:** 2345–2355.

Ishikawa, S., Hara, Y., Ohnishi, R., and Sekiguchi, J. (1998) Regulation of a new cell wall hydrolase gene, *cwlF*, which affects cell separation in *Bacillus subtilis*. *J Bacteriol* **180:** 2549–2555.

de Jong, I.G., Veening, J.-W., and Kuipers, O.P. (2010) Heterochronic phosphorelay gene expression as a source of heterogeneity in *Bacillus subtilis* spore formation. *J Bacteriol* **192:** 2053–2067.

de Jong, I.G., Beilharz, K., Kuipers, O.P., and Veening, J.-W. (2011) Live cell imaging of *Bacillus subtilis* and *Streptococcus pneumoniae* using automated time-lapse microscopy. *J Vis Exp*. DOI: 10.3791/3145.

de Jong, I.G., Veening, J.-W., and Kuipers, O.P. (2012) Single cell analysis of gene expression patterns during carbon starvation in *Bacillus subtilis* reveals large phenotypic variation. *Environ Microbiol* **14:** 3110–3121.

Kanehisa, M., Goto, S., Kawashima, S., Okuno, Y., and Hattori, M. (2004) The KEGG resource for deciphering the genome. *Nucleic Acids Res* **32:** D277–D280.

Kearns, D.B., and Losick, R. (2005) Cell population heterogeneity during growth of *Bacillus subtilis*. *Genes Dev* **19:** 3083–3094.

Kearns, D.B., Chu, F., Rudner, R., and Losick, R. (2004) Genes governing swarming in *Bacillus subtilis* and evidence for a phase variation mechanism controlling surface motility. *Mol Microbiol* **52:** 357–369.

Koburger, T., Weibezahn, J., Bernhardt, J., Homuth, G., and Hecker, M. (2005) Genome-wide mRNA profiling in glucose starved *Bacillus subtilis* cells. *Mol Genet Genomics* **274:** 1–12.

Koch, A.L. (1971) The adaptive responses of *Escherichia coli* to a feast and famine existence. *Adv Microb Physiol* **6:** 147–217.

Koch, A.L. (1997) Microbial physiology and ecology of slow growth. *Microbiol Mol Biol Rev* **61:** 305–318.

Koros, W.J., Ma, Y.H., and Shimidzu, T. (1996) Terminology for membranes and membrane processes (IUPAC Recommendation 1996). *J Membr Sci* **120:** 149–159.

Krásný, L., and Gourse, R.L. (2004) An alternative strategy for bacterial ribosome synthesis: *Bacillus subtilis* rRNA transcription regulation. *EMBO J* **23:** 4473–4483.

Lazarevic, V., Düsterhöft, A., Soldo, B., Hilbert, H., Mauël, C., and Karamata, D. (1999) Nucleotide sequence of the *Bacillus subtilis* temperate bacteriophage SPbetac2. *Microbiology* **145** (Part 5): 1055–1067.

Lendenmann, U., Snozzi, M., and Egli, T. (1996) Kinetics of the simultaneous utilization of sugar mixtures by *Escherichia coli* in continuous culture. *Appl Environ Microbiol* **62:** 1493–1499.

Lenhart, J.S., Schroeder, J.W., Walsh, B.W., and Simmons, L.A. (2012) DNA repair and genome maintenance in *Bacillus subtilis*. *Microbiol Mol Biol Rev* **76:** 530–564.

Liu, X., and Taber, H.W. (1998) Catabolite regulation of the *Bacillus subtilis ctaBCDEF* gene cluster. *J Bacteriol* **180:** 6154–6163.

Lulko, A.T., Buist, G., Kok, J., and Kuipers, O.P. (2007) Transcriptome analysis of temporal regulation of carbon metabolism by CcpA in *Bacillus subtilis* reveals additional target genes. *J Mol Microbiol Biotechnol* **12:** 82–95.

Márquez, L.M., Helmann, J.D., Ferrari, E., Parker, H.M., Ordal, G.W., and Chamberlin, M.J. (1990) Studies of sigma D-dependent functions in *Bacillus subtilis*. *J Bacteriol* **172:** 3435–3443.

Matsuoka, H., Hirooka, K., and Fujita, Y. (2007) Organization and function of the YsiA regulon of *Bacillus subtilis* involved in fatty acid degradation. *J Biol Chem* **282:** 5180–5194.

Mendez, R., Gutierrez, A., Reyes, J., and Márquez-Magaña, L. (2012) The extracytoplasmic function sigma factor SigY is important for efficient maintenance of the Spβ prophage that encodes sublancin in *Bacillus subtilis*. *DNA Cell Biol* **31:** 946–955.

Miller, J. (1972) *Experiments in Molecular Genetics*. Cold Spring Harbor, NY, USA: Cold Spring Harbor Laboratory.

Molle, V., Nakaura, Y., Shivers, R.P., Yamaguchi, H., Losick, R., Fujita, Y., and Sonenshein, A.L. (2003) Additional targets of the *Bacillus subtilis* global regulator CodY identified by chromatin immunoprecipitation and genome-wide transcript analysis. *J Bacteriol* **185:** 1911–1922.

Monod, J. (1949) The growth of bacterial cultures. *Annu Rev Microbiol* **3:** 371.

Msadek, T. (1999) When the going gets tough: survival strategies and environmental signaling networks in *Bacillus subtilis*. *Trends Microbiol* **7:** 201–207.

Muchová, K., Chromiková, Z., and Barák, I. (2013) Control of *Bacillus subtilis* cell shape by RodZ. *Environ Microbiol* **15:** 3259–3271.

Novick, A., and Szilard, L. (1950) Description of the chemostat. *Science* **112:** 715–716.

Nyström, T. (2004a) Growth versus maintenance: a trade-off dictated by RNA polymerase availability and sigma factor competition? *Mol Microbiol* **54:** 855–862.

Nyström, T. (2004b) Stationary-phase physiology. *Annu Rev Microbiol* **58:** 161–181.

Ohnishi, R., Ishikawa, S., and Sekiguchi, J. (1999) Peptidoglycan hydrolase LytF plays a role in cell separation

with CwlF during vegetative growth of *Bacillus subtilis*. *J Bacteriol* **181:** 3178–3184.

Paik, S.H., Chakicherla, A., and Hansen, J.N. (1998) Identification and characterization of the structural and transporter genes for, and the chemical and biological properties of, sublancin 168, a novel antibiotic produced by *Bacillus subtilis* 168. *J Biol Chem* **273:** 23134–23142.

Pedraza-Reyes, M., and Yasbin, R.E. (2004) Contribution of the mismatch DNA repair system to the generation of stationary-phase-induced mutants of *Bacillus subtilis*. *J Bacteriol* **186:** 6485–6491.

Petersohn, A., Brigulla, M., Haas, S., Hoheisel, J.D., Völker, U., and Hecker, M. (2001) Global analysis of the general stress response of *Bacillus subtilis*. *J Bacteriol* **183:** 5617–5631.

Piggot, P.J., and Coote, J.G. (1976) Genetic aspects of bacterial endospore formation. *Bacteriol Rev* **40:** 908–962.

Pirt, S.J. (1965) The maintenance energy of bacteria in growing cultures. *Proc R Soc Lond B Biol Sci* **163:** 224–231.

Pirt, S.J. (1982) Maintenance energy: a general model for energy-limited and energy-sufficient growth. *Arch Microbiol* **133:** 300–302.

Pirt, S.J. (1987) The energetics of microbes at slow growth rates: maintenance energies and dormant organisms. *J Ferment Technol* **65:** 173–177.

Robleto, E.A., Yasbin, R., Ross, C., and Pedraza-Reyes, M. (2007) Stationary phase mutagenesis in *B. subtilis*: a paradigm to study genetic diversity programs in cells under stress. *Crit Rev Biochem Mol Biol* **42:** 327–339.

Ryan, F.J. (1959) Bacterial mutation in a stationary phase and the question of cell turnover. *J Gen Microbiol* **21:** 530–549.

Sadaie, Y., Nakadate, H., Fukui, R., Yee, L.M., and Asai, K. (2008) Glucomannan utilization operon of *Bacillus subtilis*. *FEMS Microbiol Lett* **279:** 103–109.

Sambrook, J., Fritsch, E.F., and Maniatis, T. (1989) *Molecular Cloning: A Laboratory Manual*. Cold Spring Harbor, NY, USA: Cold Spring Harbor Laboratory.

Sauer, U., Hatzimanikatis, V., Hohmann, H., Manneberg, M., van Loon, A., and Bailey, J. (1996) Physiology and metabolic fluxes of wild-type and riboflavin-producing *Bacillus subtilis*. *Appl Environ Microbiol* **62:** 3687–3696.

Senn, H., Lendenmann, U., Snozzi, M., Hamer, G., and Egli, T. (1994) The growth of *Escherichia coli* in glucose-limited chemostat cultures: a re-examination of the kinetics. *Biochim Biophys Acta* **1201:** 424–436.

Setlow, B., Magill, N., Febbroriello, P., Nakhimovsky, L., Koppel, D.E., and Setlow, P. (1991) Condensation of the forespore nucleoid early in sporulation of *Bacillus* species. *J Bacteriol* **173:** 6270–6278.

Shivers, R.P., and Sonenshein, A.L. (2005) *Bacillus subtilis ilvB* operon: an intersection of global regulons. *Mol Microbiol* **56:** 1549–1559.

Sierro, N., Makita, Y., de Hoon, M., and Nakai, K. (2008) DBTBS: a database of transcriptional regulation in *Bacillus subtilis* containing upstream intergenic conservation information. *Nucleic Acids Res* **36:** D93–D96.

Smyth, G.K. (2004) Linear models and empirical Bayes methods for assessing differential expression in microarray experiments. *Stat Appl Genet Mol Biol* **3:** Article3.

Sonenshein, A.L. (2007) Control of key metabolic intersections in *Bacillus subtilis*. *Nat Rev Microbiol* **5:** 917–927.

Spancake, G.A., and Hemphill, H.E. (1985) Deletion mutants of *Bacillus subtilis* bacteriophage SP beta. *J Virol* **55:** 39–44.

Steil, L., Serrano, M., Henriques, A.O., and Völker, U. (2005) Genome-wide analysis of temporally regulated and compartment-specific gene expression in sporulating cells of *Bacillus subtilis*. *Microbiology* **151:** 399–420.

Stülke, J., and Hillen, W. (2000) Regulation of carbon catabolism in *Bacillus* species. *Annu Rev Microbiol* **54:** 849–880.

Tappe, W., Tomaschewski, C., Rittershaus, S., and Groeneweg, J. (1996) Cultivation of nitrifying bacteria in the retentostat, a simple fermenter with internal biomass retention. *FEMS Microbiol Ecol* **19:** 47–52.

Tatusov, R.L., Koonin, E.V., and Lipman, D.J. (1997) A genomic perspective on protein families. *Science* **278:** 631–637.

Tännler, S., Decasper, S., and Sauer, U. (2008) Maintenance metabolism and carbon fluxes in *Bacillus* species. *Microb Cell Fact* **7:** 19.

Tojo, S., Satomura, T., Matsuoka, H., Hirooka, K., and Fujita, Y. (2011) Catabolite repression of the *Bacillus subtilis* FadR regulon, which is involved in fatty acid catabolism. *J Bacteriol* **193:** 2388–2395.

Veening, J.-W., Smits, W.K., and Kuipers, O.P. (2008) Bistability, epigenetics, and bet-hedging in bacteria. *Annu Rev Microbiol* **62:** 193–210.

Veening, J.-W., Murray, H., and Errington, J. (2009) A mechanism for cell cycle regulation of sporulation initiation in *Bacillus subtilis*. *Genes Dev* **23:** 1959–1970.

van Verseveld, H.W., de Hollander, J.A., Frankena, J., Braster, M., Leeuwerik, F.J., and Stouthamer, A.H. (1986) Modeling of microbial substrate conversion, growth and product formation in a recycling fermentor. *Antonie Van Leeuwenhoek* **52:** 325–342.

Vidales, L.E., Cárdenas, L.C., Robleto, E., Yasbin, R.E., and Pedraza-Reyes, M. (2009) Defects in the error prevention oxidized guanine system potentiate stationary-phase mutagenesis in *Bacillus subtilis*. *J Bacteriol* **191:** 506–513.

Vollmer, W., Joris, B., Charlier, P., and Foster, S. (2008) Bacterial peptidoglycan (murein) hydrolases. *FEMS Microbiol Rev* **32:** 259–286.

Völker, U., Völker, A., Maul, B., Hecker, M., Dufour, A., and Haldenwang, W.G. (1995) Separate mechanisms activate sigma B of *Bacillus subtilis* in response to environmental and metabolic stresses. *J Bacteriol* **177:** 3771–3780.

Wang, S.T., Setlow, B., Conlon, E.M., Lyon, J.L., Imamura, D., Sato, T., *et al*. (2006) The forespore line of gene expression in *Bacillus subtilis*. *J Mol Biol* **358:** 16–37.

Westers, H., Dorenbos, R., van Dijl, J.M., Kabel, J., Flanagan, T., Devine, K.M., *et al*. (2003) Genome engineering reveals large dispensable regions in *Bacillus subtilis*. *Mol Biol Evol* **20:** 2076–2090.

Winstedt, L., and von Wachenfeldt, C. (2000) Terminal oxidases of *Bacillus subtilis* strain 168: one quinol oxidase, cytochrome aa_3 or cytochrome *bd*, is required for aerobic growth. *J Bacteriol* **182:** 6557–6564.

Winstedt, L., Yoshida, K., Fujita, Y., and von Wachenfeldt, C. (1998) Cytochrome *bd* biosynthesis in *Bacillus subtilis*: characterization of the *cydABCD* operon. *J Bacteriol* **180:** 6571–6580.

Yamamoto, H., Kurosawa, S., and Sekiguchi, J. (2003) Localization of the vegetative cell wall hydrolases LytC, LytE, and LytF on the *Bacillus subtilis* cell surface and stability of these enzymes to cell wall-bound or extracellular proteases. *J Bacteriol* **185:** 6666–6677.

Yeom, S.-J., Ji, J.-H., Kim, N.-H., Park, C.-S., and Oh, D.-K. (2009) Substrate specificity of a mannose-6-phosphate isomerase from *Bacillus subtilis* and its application in the production of L-ribose. *Appl Environ Microbiol* **75:** 4705–4710.

Zhang, S., and Haldenwang, W.G. (2005) Contributions of ATP, GTP, and redox state to nutritional stress activation of the *Bacillus subtilis* sigmaB transcription factor. *J Bacteriol* **187:** 7554–7560.

Supporting information

Additional Supporting Information may be found in the online version of this article at the publisher's web-site:

Fig. S1. Distribution of glucose (%) between maintenance and growth. Black bars represent energy directed towards maintenance ($m_s \cdot C_{x,viable}$). White bars represent energy directed towards growth ($\mu \cdot C_{x,viable}/Y_{sx}^{max}$). (A) Retentostat 1. (B) Retentostat 2.

Table S1. Highly differentially expressed genes in response to near-zero growth conditions.

Table S2. SNPs resulting in missense mutations.